

Babes-Bolyai University
Faculty of Chemistry and Chemical Engineering

PhD THESIS ABSTRACT

**PHOTOCATALYSTS BASED ON DOPED AND
UNDOPED TiO₂ AEROGELS.
CHARACTERIZATION AND APPLICATIONS.**

**Scientific supervisor,
Prof. Dr. Ionel Catalin Popescu**

**PhD student,
Popa Mihaela**

2010

TABLE OF CONTENTS

INTRODUCTION

Cap.1. PHOTOCATALYSTS BASED ON DOPED TiO₂ AEROGELS

- 1.1. Aerogels. Generalities
 - 1.1.1. Aerogels applications
 - 1.1.2. The synthesis of TiO₂ aerogels
- 1.2. Doped TiO₂ photocatalysts
 - 1.2.1. Morphostructural and optical properties of TiO₂
 - 1.2.2. Metal doped TiO₂
 - 1.2.3. Non-metal doped TiO₂

Cap. 2. THE APPLICATION OF DOPED TiO₂ IN PHOTOCATALYSIS

- 2.1. Heterogeneous photocatalysis
 - 2.1.1. The principal of heterogeneous photocatalysis
 - 2.1.2. Important parameters in photocatalysis
- 2.2. Organic compounds photocatalysis using doped TiO₂ photocatalysts
 - 2.2.1. Aliphatic pollutants photooxidation
 - 2.2.2. Aromatic and haloaromatic pollutants photooxidation
 - 2.2.3. Dye pollutants photooxidation
- 2.3. Hydrogen production by photocatalysis

Cap.3. MATERIALS AND TECHNIQUES USED

- 3.1. Materials
- 3.2. Techniques and working conditions

Cap.4. PHOTOCATALYSTS BASED ON TRANSITION METAL DOPED TiO₂ AEROGELS

- 4.1. Introduction
- 4.2. The synthesis of transition metal doped TiO₂ aerogels
- 4.3. The morphostructural characterization of the undoped and metal doped TiO₂ aerogels
 - 4.3.1. The influence of Fe (III), Ce (II), Cu (II) ions on the morphostructural properties of TiO₂
 - 4.3.2. The influence of Fe (III) ions concentration on the morphostructural properties of TiO₂
- 4.4. Photocatalytic activity estimation of the metal doped TiO₂ aerogels
 - 4.4.1. Salicylic acid adsorption of the photocatalyst surface
 - 4.4.2. Salicylic acid photodegradation
 - 4.4.3. The influence of the specific surface area on the photocatalytic activity
- 4.5. Conclusions

Cap.5. PHOTOCATALYSTS BASED ON NON-METAL DOPED TiO₂ AEROGELS (TiO_{2-x}N_x)

- 5.1. Introduction
- 5.2. The synthesis of nitrogen doped TiO₂ aerogels
 - 5.2.1. Doping with nitrogen
 - 5.2.2. Thermal treatment
- 5.3. Elemental and morphostructural characterization on N doped TiO₂ aerogels
- 5.4. Photocatalytic activity estimation of N doped TiO₂ aerogels
 - 5.4.1. Salicylic acid adsorption on the photocatalyst surface

5.4.2. Salicylic acid photodegradation

5.5. Conclusions

Cap. 6. Fe³⁺-TiO₂ AND TiO_{2-x}N_x APPLICATION ON POLLUTANT ORGANIC COMPOUNDS

PHOTODEGRADATION

6.1. Introduction

6.2. Organic compounds photodegradation

6.2.1. Photocatalysts

6.2.2. Working conditions

6.2.3. The evaluation of the photooxidized organic compounds by GC-MS

6.3. Conclusions

Cap.7. PHOTOCATALYSIS H₂ PRODUCTION USING Pt/N-TiO₂ AEROGELS

7.1. Introduction

7.2. The synthesis of Pt/undoped and nitrogen doped TiO₂ aerogels

7.3. The morphostructural characterization of Pt/ undoped and nitrogen doped TiO₂

7.4. Photocatalytic activity estimation of N doped TiO₂ aerogels

7.5. Hydrogen production using Pt/ undoped and nitrogen doped TiO₂ aerogels

7.6. Conclusions

GENERAL CONCLUSIONS

REFERENCES

ACKNOWLEDGEMENTS

Anexes

Keywords: TiO₂, transition metal, nonmetal, doping, aerogel, photocatalysis, wastewater pollutants, hydrogen production via photocatalysis

ABBREVIATIONS

Fe – iron
Cu – copper
Ce – cerium
N - nitrogen
TIP- titanium tetraizopropoxide
ETOH – ethanol
H₂O – water
HNO₃ – nitric acid
Me-TiO₂ – metal doped TiO₂
N-TiO₂ – nitrogen doped TiO₂
CO₂ – carbon dioxide
ICP-MS - inductively coupled plasma-mass spectrometry
DRS – diffuse reflectance spectroscopy
XRD- X ray diffraction
TEM/SAED – transmission electron microscopy/ selected area electron diffraction
SEM – scanning electron microscopy
[OH_{surf}] – concentration of surface OH groups
UV – ultraviolet radiation /ultraviolet domain
VIS – visible radiation / visible domain
XPS- X ray photoelectron spectroscopy
S_{BET} – specific surface area
Conc.- concentration
GC-MS – gas chromatography coupled by mass spectrometry
SA – salicylic acid
FTIR – Fourier transformed infrared spectroscopy
Pt – Platinum

INTRODUCTION

Nowadays the environmental protection is one of the most important objectives of the humanity. A lot of techniques are employed to accomplish this task. Among these, photocatalysis is a promising method used in degradation of different water or air organic pollutants. The principle of photocatalysis involves the mineralization of organic compounds till CO₂ and H₂O by using the UV (VIS) irradiation of the photocatalyst.

Regarding its properties, TiO₂ is considered a very suitable photocatalyst. It is a nontoxic material, with chemical stability, low cost and high oxidation power. TiO₂ is a semiconductor with a band gap of about 3.2 eV allowing absorption of UV light (about 5% of solar spectrum). However, the absorption of only a small fraction of the solar spectrum makes TiO₂ not enough efficient for practical applications. Additionally, the electron-hole recombination is considered a serious problem for its photocatalytic performances, since this process limits severally the TiO₂ quantum yield.

Doping TiO₂ with transition metals has been considered an efficient method for extending the TiO₂ absorption in visible region of solar spectrum. At the same time, it was stated that doping metals create localized states in TiO₂ band gap, acting as electron/hole traps. However, the beneficial effect of metal doping is still uncertain, being sometimes accepted or rejected.

Cu doped TiO₂ xerogels has been traditionally used for CO₂ photocatalytic reduction process, but few studies were dedicated to photo-oxidation processes.⁹⁻¹¹ Thus, in comparison with undoped TiO₂, Cu-TiO₂ xerogels, synthesized by sol-gel process, showed an enhanced photocatalytic activity for methylene-blue photo-oxidation.⁴⁹ Ce and Fe doped TiO₂ xerogels were more frequently investigated, but their effect on the photocatalytic activity still remains a controversial subject. Fe doped TiO₂ showed a higher photocatalytic activity for phenol, methanol, methyl orange and cyclohexane photodegradation, than that observed for undoped TiO₂^{65, 122, 123, 126, 127, 129}. Similarly, Ce doped TiO₂ showed a better efficiency for formaldehyde¹⁰¹ and 4-chlorophenol³⁸ photodegradation. In the case of TiO₂, it was found that the optimum concentration of metal doping is placed in the range of 0.5 - 1 at %. At the same time, it was reported that: (i) Fe doped TiO₂ decrease the TiO₂ photocatalytic activity for methylene blue and benzoic acid degradation¹²⁰⁻¹²²; (ii) Ce doped TiO₂ presents lower photoactivity for rhodamine B¹³⁷ photodegradation than undoped TiO₂.

The beneficial effect of nitrogen on the photocatalytic activity of TiO₂ was described for the first time by Asahi et al. Subsequent studies reported that nitrogen doped TiO₂ exhibit absorption in the visible region and showed an enhanced photocatalytic activity under visible light irradiation. In the last years the chemical nature of nitrogen doping centers and their influence on the band structure of TiO₂ were also thoroughly investigated. All results lead to the conclusion that nitrogen effect on TiO₂ depends on many factors: the synthesis procedure (sol-gel, ion implantation, magnetron sputtering, oxidation of titanium nitride etc.), the location of nitrogen species (NO_x, substitutional N or NH_x) in the TiO₂ structure, the interaction between the N centers and oxygen vacancies etc^{76, 78, 83, 85, 88, 90, 162, 163}.

Generally, it was concluded that the photocatalytic efficiency of metal doped TiO₂ is strongly dependent on the conditions of preparation, on their morphostructural properties (crystalline structure, specific surface area, and surface OH group's concentration) and on the type of the organic pollutant photooxidized.

It was noticed that by increasing the specific surface area (~ 150 m²/g) and the surface OH group's concentration, the pollutant adsorption and photodegradation efficiency on the titania based photocatalyst increase.⁶⁹ Titania aerogels combine the aerogel properties (high porosity and high surface area) with those of the TiO₂.

Taking into account that, it was considered interesting to correlate the synthesis conditions (especially the doping procedure, the temperature and time of thermal treatment) with the morpho-structural properties and the UV-VIS photocatalytic activity of the Fe-, Ce-, Cu- and N-doped TiO₂ aerogels.

The thesis consists in seven chapters from which two of them are dedicated to theoretical aspects, closely related to the aim of the work, one refers to the materials and the technique used to obtain and characterize the prepared materials and the last four chapters refers to the original contribution in this field.

4. PHOTOCATALYSTS BASED ON TRANSITION METAL DOPED TiO₂ AEROGELS

The aim of this study was to obtain Fe-, Ce-, Cu-doped TiO₂ aerogels and to investigate the influence of the type and the concentration of the doping metal on morpho-structural properties and to test the salicylic acid photodegradation efficiency, respectively.

4.1. Synthesis conditions

Sol-gel process followed by supercritical drying with CO₂ was employed in order to obtain the metal doped TiO₂ aerogels. Doping agents were: Fe(NO₃)₃·9H₂O, Ce(NO₃)₂·6H₂O, Cu(NO₃)₂·3H₂O which were added during the sol-gel synthesis. The molar ratios of the sol-gel reactants and the doping agents are mentioned in the below table (Table 4.2).

Table 4.2. Molar ratios of the sol-gel reactants and of the doping agent.

Solution	Solution components	Molar ratio
Me (Fe / Ce / Cu) -TiO ₂	[Me(NO ₃) _x] : [TIP]	0.015
	[ETOH]:[TIP]	21
	[H ₂ O]: [TIP]	3.675
	[HNO ₃]: [TIP]	0.08 (pH = 4.0)
	Gelling time (min) :	5-7
Experimental conditions		
Reaction time (min) / Reaction temperature (°C)		7 /20

A set of Fe (0.4-1.8 % at) -TiO₂ gels were prepared in the same conditions mentioned in the table 4.2 except that the concentration of doping agent (Fe(NO₃)₃·9H₂O) was varied (Table 4.3).

The supercritical drying with CO₂ of TiO₂ gels was performed in a critical point dryer (SAMDRI-PVT 3D, Tousimis), 1h maintained in supercritical conditions (100 atm, 40 °C).

Table 4.3. Precursors molar ratio and iron content

Sample notation	Sample content	Molar ratio Fe(NO ₃) ₃ / TIP	Molar ratio ETOH/TIP	Fe theoretical content (% at)	Fe determined content ^a (% at)
(A)	Fe-TiO ₂	0.03	21	2	1.8
(B)		0.015	17.45	1	0.9
(C)		0.0075	21	0.5	0.45
(D)		0.03	17.45	2	1.8
(E)		0.0075	17.45	0.5	0.45

^a ICP-MS determinations

The obtained aerogels were thermal treated at 500°C for 2h in air, and then were morpho-structural characterized.

4.2. Optical and morphostructural characterization

4.2.1. Influence of the doping metal on the TiO_2 aerogel characteristics

4.2.1.1. Optical characteristics

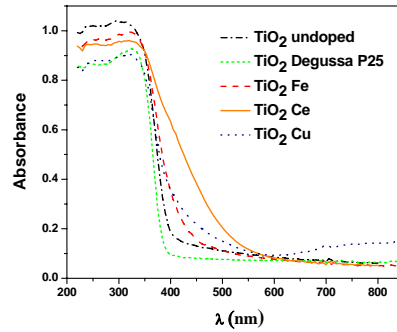


Fig. 4.1. UV-Vis diffuse reflectance spectra for doped, undoped TiO_2 and Degussa P25 samples

Ce doped TiO_2 shows a large range of absorption in the visible region (around 525 nm). Cu doped TiO_2 presents absorption around 408 nm and also over 600 nm of the visible region. The band located at 400-500 nm might be assigned to three-dimensional Cu^+ clusters existing in the CuO matrix. The adsorption bands at 600-800 nm are assigned to $2\text{E}_g \rightarrow 2\text{T}_{2g}$ transitions of Cu^{2+} . Among the doped samples, Fe doped TiO_2 exhibits the smallest absorption in the visible range (around 451 nm).

4.2.2. Morpho-structural characteristics

Anatase (tetragonal $D_{4h}\text{I}4_1/\text{amd}$) was the main crystalline phase of all the investigated samples. However, brookite and rutile phases are also present. The highest amount of anatase was found in Fe doped (96.3%) and Ce doped TiO_2 (95%). The formation of brookite phase seems to be favoured in the undoped and Cu doped TiO_2 aerogel. The presence of Cu favours the formation of rutile phase too.

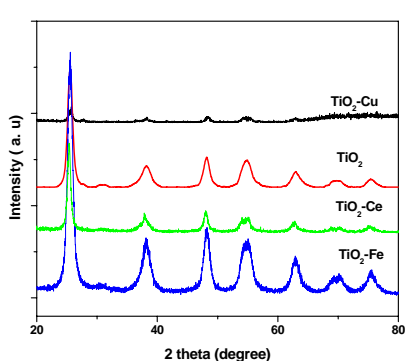


Fig.4.2. XRD spectra of the obtained aerogel samples

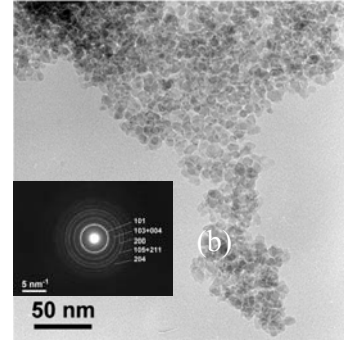


Fig.4.7. TEM/SAED image of Fe (0.7at %)- TiO_2 aerogel

The TEM measurements revealed the presence of nanometric particles with mean particle size of 10-14 nm (Fig. 4.7 and 4.8).

The adsorption-desorption isotherms of the type IV with the H2 hysteresis loop (Fig.4.10) indicates a complex pore structures which tends to be made up of interconnected networks of pores of different size and shape.

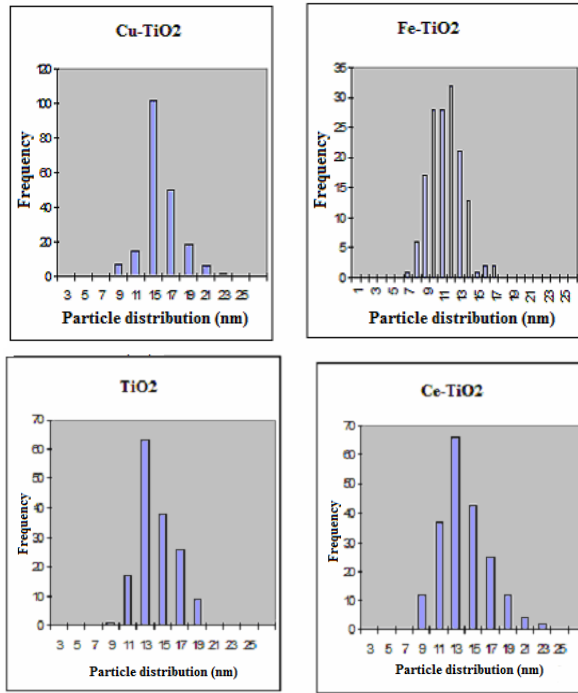


Fig.4.8. Particles size distribution of undoped TiO_2 (13.3 ± 2.2 nm), TiO_2 -Ce (12.8 ± 2.8 nm), TiO_2 -Cu (14.1 ± 2.9 nm), TiO_2 -Fe (10.8 ± 1.8 nm) determined by TEM

The undoped TiO_2 aerogel exhibits the highest mesopores volume, while mesopores volume of Fe-TiO₂, Ce-TiO₂ and Cu-TiO₂ was 1.46, 1.88, and, respectively, 1.40 times smaller. S_{BET} of the metal doped TiO_2 aerogels was almost unchanged in the case of Fe doped TiO_2 , but it decreased 1.63 times for Ce doped TiO_2 and 1.24 times for Cu doped TiO_2 . Metal doping of TiO_2 induces a decreasing of the pore volume and specific surface area.

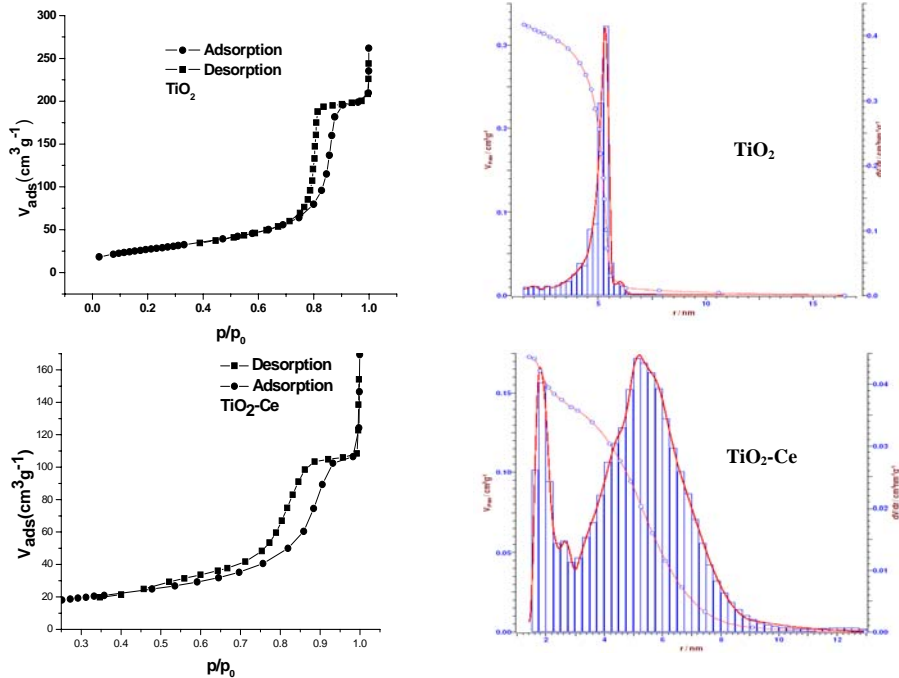


Fig.4.10. Adsorption-desorption isotherms and pores size distribution of undoped and Ce doped TiO_2 aerogels

4.2.2. Influence of metal (Fe ions) concentration on TiO_2 aerogel characteristics

The XPS spectra (Fig.4.11) reveal the presence of Fe^{3+} ions (indicated by the ~ 710 eV și ~ 723.6 eV peaks) in TiO_2 lattice as Fe-O-Ti or Fe_2O_3 . Some Fe^{2+} traces in TiO_2 lattice can be evidenced by the presence of the satellite peak at ~ 714 eV.

XRD diffractograms (Fig.4.14) indicate mainly the presence of anatase structure. The brookite crystalline structure was increasing (from 13% to 28%) by increasing the iron concentration from 0.4-1.8 at %.

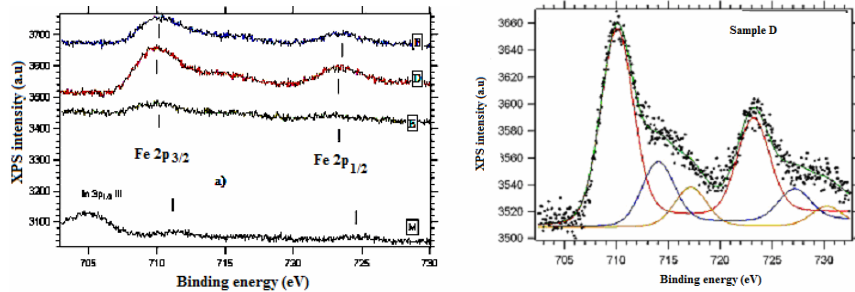


Fig.4.11. XPS spectra of the Fe (0.4-1.8 at %)- TiO_2 aerogels

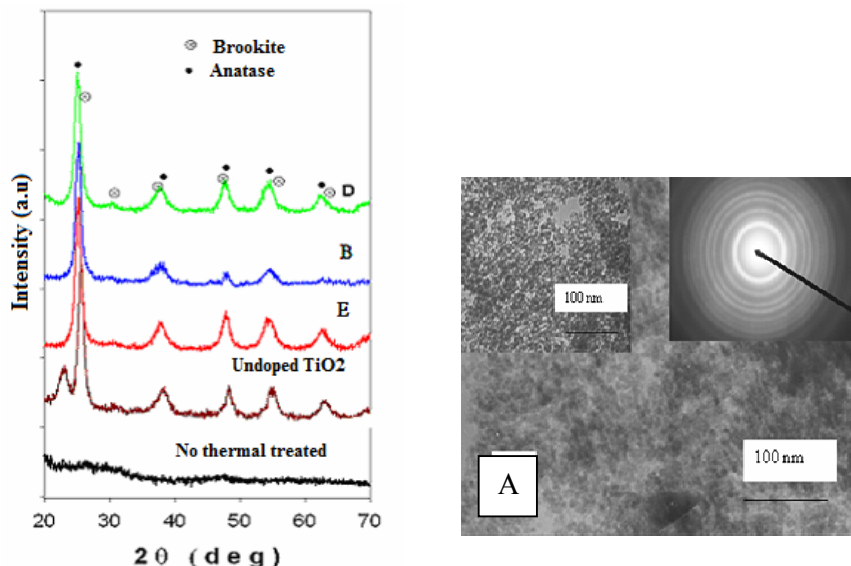


Fig. 4.14. XRD diffractograms of the undoped, (B) Fe (0.9 at%) - TiO_2 , (D) Fe (1.8 at %) TiO_2 , (E) Fe (0.4 at%)- TiO_2

Fig.4.16. TEM/SAED image of sample A (1.8 % at)

The mean anatase particle size of the Fe (0.4-1.8 at %) were around 9-13 nm. Generally, only mezopores having sizes between 10-30 nm were observed and the minimal size of detected pores was similar to the mean size of anatase nanoparticles. The porosity can be changed as a function of iron doping. Thus, in the sample C, which has a minimal iron content, a high and interconnecting porosity was detected, while the sample B, which is very compact, contains a major fraction of individual pores, without intercommunicate ion among them. A peculiar structure is registered for the highest iron content (specimen A) (Fig. 4.16) where the microporosity was found to increase; a circumferential and interconnecting porosity around anatase particles can be observed.

4.3. Photocatalytic activity estimation of metal doped TiO_2 aerogels

The photocatalysts were UV-VIS irradiated during 120 min using salicylic acid ($5 \cdot 10^{-4}$ M), as a standard pollutant. To evaluate the photocatalytic activity of the doped, undoped TiO_2 aerogels and TiO_2 Degussa powder, the

dependence $\ln(C_0/C)$ vs. time was recorded. The apparent rate constant (k_{app}) of the salicylic acid photodegradation was taken as the slope of the $\ln(C_0/C)$ vs. time plot. The evaluation of photocatalytic activity of the samples correlated with radiation intensity was performed by determining the photonic efficiency (ξ).

Adsorption of the salicylic acid on Me-TiO₂ surface was performed and it was found to increase by increasing the specific surface area and [OH_{surf}] (Fig. 4.20)

Among the metal doped TiO₂ samples, the highest value of the apparent rate constant was observed for Fe doped TiO₂ (table 4.7). In order to estimate the effect of metal doping on the photocatalytic activity of TiO₂ aerogels, eliminating the differences existing between the S_{BET} values, the k_{app}/S_{BET} ratio was calculated. It was found that **Ce doped TiO₂** exhibits the highest value of k_{app}/S_{BET} ratio. Despite of its small S_{BET} and mesopores volume, it has a high percentage of anatase (94.9 %), a high amount of OH surface groups (regarding the doped TiO₂ series), a high mesopores radius and its band gap is ~2.37 eV which allows it to absorb VIS light.

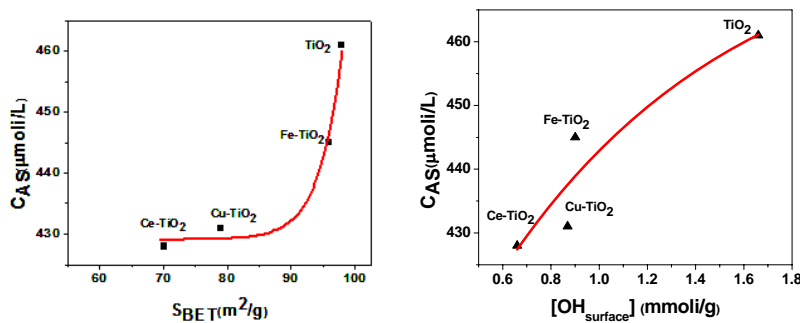


Fig.4.20. Salicylic acid adsorption as function of specific surface area (left) and surface OH groups concentration (right)

Table 4.7. Porosity characteristic, apparent rate constant and photonic efficiency

Sample	Mean mesoporous radius (nm)	Mesoporous Volume (cm ³ /g)	[OH _{surf}] (mmol/m ²)	S _{BET} (m ² /g)	k _{ap} 10 ³		k _{ap} /S _{BET} (g/m ² min)	ξ (10 ⁴)
					(min ⁻¹)	R		
TiO ₂	5.18	0.32	0.017	98	10.5	0.992	0.071	1.20
Fe-TiO ₂	3.12	0.22	0.009	96	9.8	0.993	0.102	1.30
Ce-TiO ₂	5.09	0.17	0.011	60	9.7	0.996	0.191	1.29
CuTiO ₂	4.69	0.23	0.011	79	6.9	0.990	0.087	1.07
TiO ₂ Degussa	6.9	-	0.011	42	3.5	0.983	0.083	0.50

Increasing the iron concentration from 0.4 to 1.8 at % a maximum of photocatalytic activity was observed (table 4.8) for salicylic acid.

Table 4.8. Specific surface area, apparent rate constant and photonic efficiency of Fe (0.4-1.8 at %) – TiO₂

Sample	S _{BET} (m ² /g)	k _{ap} 10 ³		k _{ap} /S _{BET} (g/m ² min)	ξ (10 ⁴)
		(min ⁻¹)	R		
A	163	14.9	0.994	0.091	1.59
B	141	13.1	0.995	0.092	1.50
C	125	9.3	0.992	0.074	1.35
D	143	14.7	0.990	0.102	1.55
E	139	9.6	0.998	0.069	1.32
TiO ₂ undoped	130	12.5	0.994	0.071	1.47
Degussa P25	42	3.5	0.983	0.083	0.50

Cap.5. PHOTOCATALYSTS BASED ON NON-METAL DOPED TiO₂ AEROGELS (N-TiO₂)

The aim of this study was to obtain N doped TiO₂ aerogels, using different nitrogen sources, different methods of doping and different times and temperatures of thermal treatment. The as-prepared photocatalysts were characterized and then were tested for salicylic acid photodegradation.

5.1. Synthesis conditions

The sol-gel process, using the reactants mentioned in table 4.2, was employed in order to obtain the N-TiO₂ aerogels. The nitrogen sources were: urea, NH₃ (25%) solution and guanidine-HCl. Four methods of doping were used:

(A) – urea added during the sol-gel synthesis; (B) – TiO₂ gel immersed in NH₃ sol.; (C) – TiO₂ aerogel immersed in NH₃ sol.; (D) urea added during the synthesis and the obtained aerogel was immersed in NH₃ sol.

The obtained samples were thermal treated from 450 to 550°C and the time of thermal treatment was from 10, 60 (table 5.2) and 120 min.

Table. 5.2. Doping method, time and thermal treatment of the N-TiO₂ aerogels

Sample TiO _{2-x} N _x	Doping method	Temperature of thermal treatment [°C]	Time of thermal treatment [min]
A	Undoped TiO ₂ aerogel	530	10
B	A	530	10
A530-10		530	10
A550-10	C	550	10
A450-10		450	10
A450-60		450	60
B530-10	D	530	10
G530-10	B	530	10

5.2. Morpho-structural characteristics

5.2.1. Optical characteristics

Adding urea in synthesis (urea/TIP molar ratio = 0.025-0.102) do not produce adsorption in the VIS region (Fig. 5.2.b). Absorption in the VIS region, with a maximum at ~ 430 nm, was noticed by doping using B, C, D methods.

5.2.2. Structural characteristics

1) The XRD patterns (Fig.5.5) support the conclusion that all samples obtained under this synthesis conditions have mainly a crystalline structure corresponding to tetragonal anatase.

The values of the anatase particles size are relatively high (15-22 nm) due to the short time (10 min) of the thermal treatments. The thermal treatment of about 1 hour at 450°C decreases the mean size of the anatase particles with about 55%, the sample (A450-60) have the smallest anatase particle size (10 nm).

2) The XPS measurements indicate the presence of substitutional N (398 eV), interstitial N (401 eV) and possible some adsorbed NO, NH₃ species or interstitial N (400 eV) in TiO₂ lattice (Fig.5.8).

3) FTIR analysis indicate the decreasing of surface OH groups by immersing

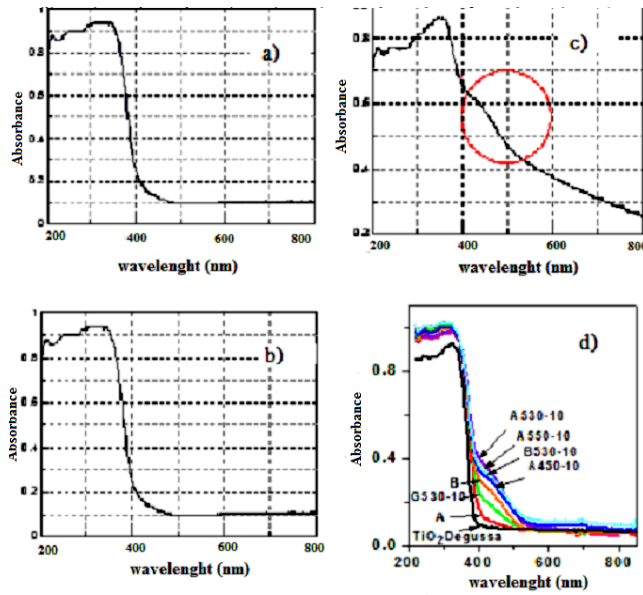


Fig. 5.2. Diffuse reflectance spectra for a) the undoped TiO_2 , b) $\text{N}-\text{TiO}_2$ (method A, $500^\circ\text{C}/120$ min), c) $\text{N}-\text{TiO}_2$ (method C, $500^\circ\text{C}/120$ min), d) $\text{N}-\text{TiO}_2$ (different methods, times and temperatures of thermal treatment (table 5.2))

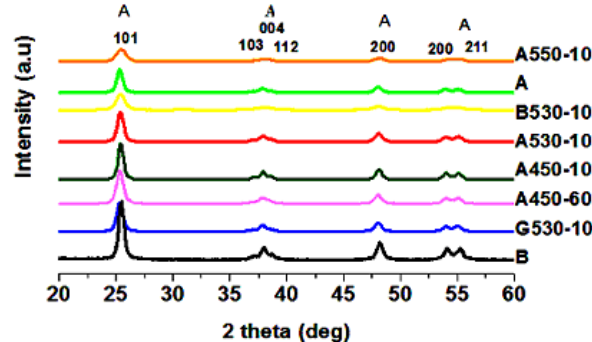


Fig. 5.5. XRD diffractograms of the samples mentioned in table 5.2

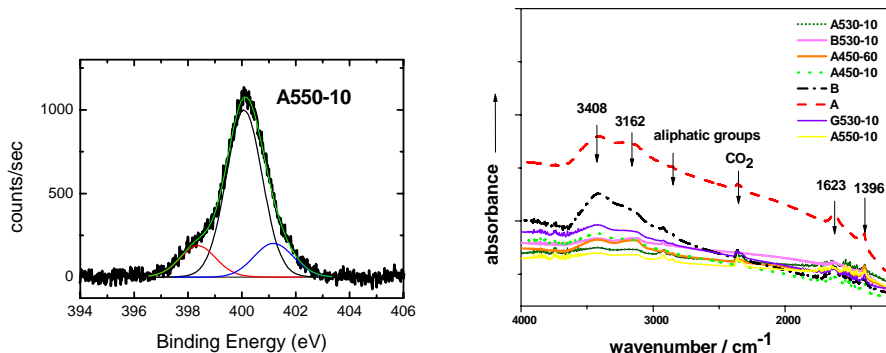


Fig. 5.8. XPS spectra of sample A530-10.

Fig. 5.12. FTIR spectra of samples presented in table 5.2.

TiO_2 aerogel in NH_3 sol. but do not indicate a sure evidence of the presence of N species on the surface of TiO_2 regarding NH_3 immersion. The peak at 1398 cm^{-1} could be attributed to the presence of hyponitrite (N_2O_2)²⁻. The presence of this peak in the bare TiO_2 as well makes implausible this assumption, considering NH_3 as a generating source. The nitric acid, used as acid catalyst during the synthesis process, could be a more reliable source for hyponitrite formation.

5.2.3. Pores characterization

A representative adsorption-desorption isotherm is presented in Fig. 5.10. A decreasing of the porosity and S_{BET} of the NH_3 immersed TiO_2 aerogels can be observed in the NH_3 sol. immersed samples. NH_3 solution has a collapsing effect on the TiO_2 aerogel structure. A higher S_{BET} of the sample *G530-10*, comparing with the rest of the NH_3 impregnated samples, could be explained by the fact that the TiO_2 wet gel was immersed in NH_3 solution and thus, the collapsing effect on aerogel structure was diminished.

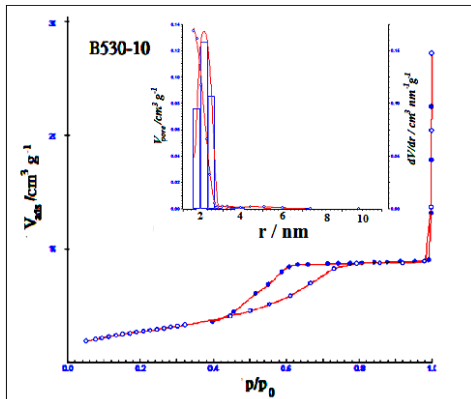


Fig.5.10. Adsorption-desorption isotherms and pore size distribution of sample B530-10

5.3. Photocatalytic activity estimation of the nitrogen doped TiO_2

Photonic efficiency (ξ) was determined in order to evaluate the photocatalytic activity of the samples (Table 5.7).

The photocatalytic activities of the samples *A530-10*, *B530-10*, *A450-60*, *G530-10*, *A550-10* are higher with respect to the undoped TiO_2 (sample *A*).

Table. 5.7. Band gap, pores characteristics, $[\text{OH}_{surf}]$, S_{BET} and photonic efficiency

Catalyst	Band gap (eV)	Mesopores mean radius (nm)	Pores volume (cm^3/g)	$[\text{OH}_{surface}]$ (mmol/g)	S_{BET} (m^2/g)	ξ (10^4)
A	3.04	4.5	0.5	0.70	131	1.01
B	2.97	4.9	0.4	0.69	103	1.06
A530-10	2.80	2.1	0.1	0.57	67	1.26
A550-10	2.84	2.1	0.1	0.55	71	1.08
A450-10	2.80	1.9	0.2	0.64	91	0.99
A450-60	2.82	2.1	0.1	0.65	99	1.22
B530-10	2.86	2.0	0.1	0.38	78	1.32
G530-10	3.02	4.6	0.3	0.71	105	1.26
TiO ₂ Degussa (P25)	3.23	6.9	-	0.11	42	0.50

The samples *A530-10*, *G530-10* and *B530-10* exhibit the highest photocatalytic activity among the N-TiO₂ samples. A high amount of nitrogen incorporated in substitutional and interstitial positions of TiO₂ lattice, a higher S_{BET} led to the highest photocatalytic activity ($\xi = 1.32 \cdot 10^4$) of sample *B530-10*. Sample *A530-10* exhibits a slightly smaller photoactivity than sample *B530-10*, in contrast with its higher number of surface OH groups, smaller anatase particle size and higher microstrain, respectively. Sample *G530-10* is a particular case. In spite of many favorable factors (~1.63 times smaller particle size, higher porosity and surface area than sample *B530-10*, the highest surface OH concentration among of all the investigated samples), it did not show the highest photocatalytic activity. Urea addition in TiO₂ synthesis (sample *B*) showed unnoticeable increase of the photocatalytic activity, with respect of

undoped TiO₂. The photocatalytic activity of the sample *B* increases about 1.3 times after its immersion in NH₃ solution (sample *B530-10*), reported to the undoped TiO₂. A maximum of photocatalytic activity was obtained by increasing the temperature from 450°C (10 min) to 530°C (10 min). The lowest photocatalytic activity of the sample *A450-10* might be due to its highest particle size (22 nm) comparing with the rest of the samples.

VIS irradiation (using 4 R7S fluorescent lamps (24W)) of the A530-10 photocatalyst during 135 min decreases SA concentration with about 31.7% (Fig.5.17).

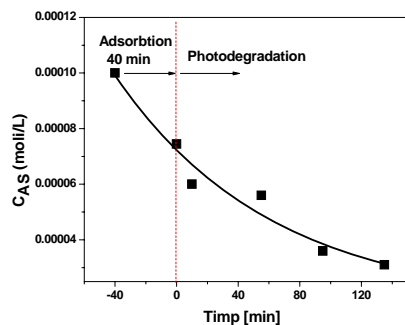


Fig.5.17. The decreasing of the SA concentration by VIS irradiation

Cap.6. Fe³⁺-TiO₂ AND TiO_{2-x}N_x APPLICATION ON POLLUTANT ORGANIC COMPOUNDS PHOTODEGRADATION

In this study Fe (1.8 at %)-TiO₂, N-TiO₂, undoped TiO₂ aerogels and TiO₂ Degussa P25 were tested at UV (312 nm) photooxidation of some pollutant organic compounds: 2, 6 – dichlorphenol, 1,2,3-trichlorbenzene, ametrine, triclosan

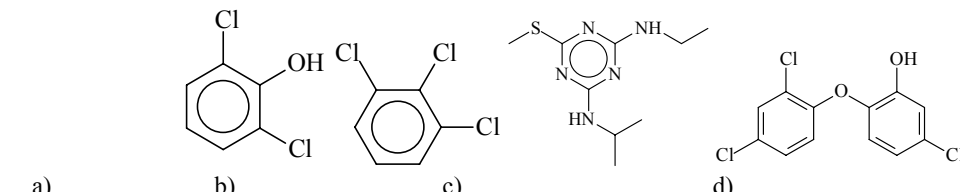


Fig.6.1. Organic compounds: a) 2,6 – dichlorphenol ($M=162$), b) 1,2,3 – trichlorbenzene ($M=180$), c) ametrine ($M=227$), d) triclosan ($M=288$)

Table.6.1. Final concentration and percents of photodegraded organic compounds, after 5 hour of UV irradiation, using different photocatalysts (initial concentration 200 µg/L)

Nr. Prb.	Photocatalyst	Organic compound	Final Conc. [µg/L]	Compound transformed [%]
1.	M (TiO ₂)	2,6-dichlorfenol	1.05	99.5
		1,2,3-trichlorbenzene	0.78	99.6
		Ametrine	0.78	99.6
		Triclosan	0.20	99.9
2.	A (Fe(1.8at%)-TiO ₂)	2,6-dichlorfenol	1.17	99.4
		1,2,3-trichlorbenzene	1.74	99.1
		Ametrine	1.14	99.4
		Triclosan	0.31	99.8
3.	A2 (N (0.5%)-TiO ₂)	2,6-dichlorfenol	0.78	99.6
		1,2,3-trichlorbenzene	1.06	99.5
		Ametrine	0.72	99.6
		Triclosan	0.28	99.8
4.	DP25	2,6-dichlorfenol	1.85	99.1
		1,2,3-trichlorbenzene	0.72	99.6
		Ametrine	1.63	99.2
		Triclosan	0.63	99.7

The adsorption of the organic compounds on the photocatalyst was depending on the hydrophilicity of the compound and the specific surface area of the photocatalyst. Thus, for the hydrophilic compounds (ametrine) the adsorption was ~ 45% while for the hydrophobic compounds (2,6 – dichlorphenol, 1,2,3 –trichlorbenzene, triclosan), the adsorption was ~ 70%. Monitoring the remaining compounds by GC-MS, after 5 hours of UV irradiation the organic compounds were > 99% adsorbed and photodegraded.

Cap.7. PHOTOCATALYSIS H₂ PRODUCTION USING Pt/N-TiO₂ AEROGELS

Platinum was photodeposited on undoped TiO₂ and N-TiO₂ aerogels and TiO₂ Degussa P25 in order to test them for hydrogen production via photocatalysis.

7.1. Synthesis condition

N doped TiO₂ aerogels were obtained by sol-gel process and supercritical drying with CO₂, except that TIP was refluxed with the nitrogen source (urea, guanidine-HCl) during the sol-gel synthesis (Table 7.1.).

Table 7.1. Molar ratios between nitrogen source and TIP

Sample	[UREE]/[TIP]	[GUAN]/[TIP]
I	0.24	-
II	0.37	-
III	0.48	-
IV	0.12	-
V	-	0.08
VI	-	0.16
VII	-	0.23
VIII	-	0.28

The obtained aerogels were thermal treated at 530°C/10 min or 500°C/120 min.

Pt (~1%) was photodeposited on the obtained aerogels, undoped TiO₂ aerogels and TiO₂ Degussa P25, using an aqueous solution of (C₂H₂O₄) ($5 \cdot 10^{-3}$ M) and H₂PtCl₆ ($3.56 \cdot 10^{-5}$ M) and UV irradiation.

7.2. Structural characterization

The crystalline structure of the Pt/N-TiO₂ (530°C/10 min) aerogel is mainly anatase. The mean particles size was about 11-24 nm, with the highest particle size for the Pt/VIII aerogel.

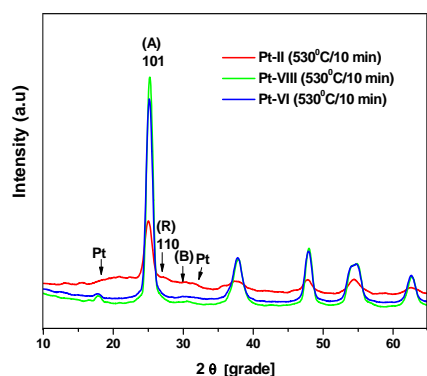


Fig.7.3. XRD spectra of Pt/N-TiO₂ aerogels

7.3. Pores characterization

The process of Pt deposition on the surface of the aerogels determined a decreasing of the pores volume, mean mesopores size and specific surface area. In the case of sample VIII, Pt deposition produced a decreasing with about 67.5% and 35.44% of the pores volume and specific surface area, respectively (Fig.7.6).

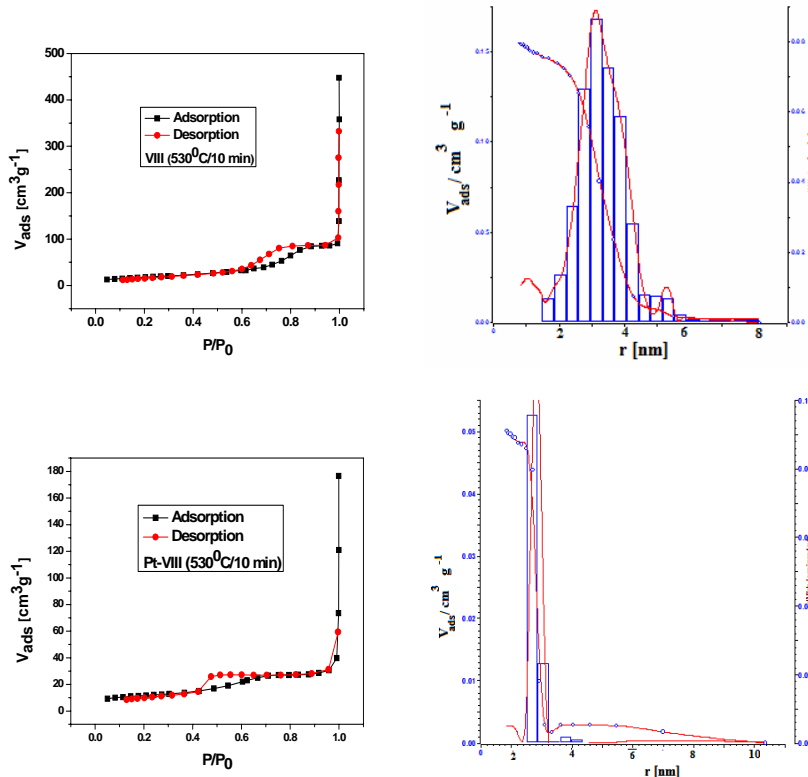


Fig. 7.6. Adsorption-desorption isotherms and pores size distributions of samples VIII and Pt/VIII

7.4. Hydrogen production using Pt/ undoped and nitrogen doped TiO₂ aerogels

As can be observed in Fig. 7.8, in the absence of a sacrificial agent (oxalic acid) the hydrogen production rate is $\sim 0.23 \mu\text{mol}/\text{min}$. In the presence of the oxalic acid ($5 \cdot 10^{-4} \text{ M}$), the hydrogen production rate increase with about 97%, using a temperature of 25°C and Pt/undoped TiO₂ aerogel. Increasing the temperature from 25°C to 75°C the hydrogen production rate increased again about 26%.

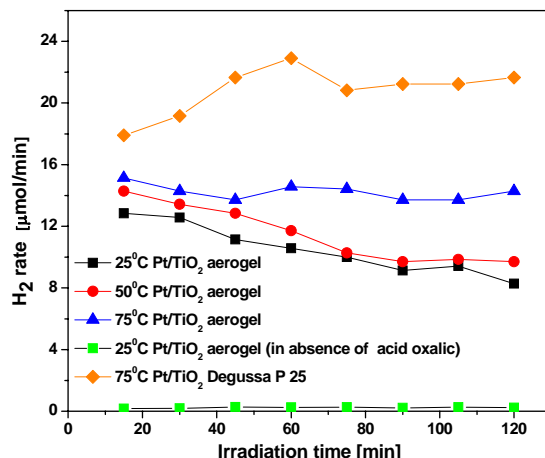


Fig.7.8. Hydrogen production at different temperatures of reaction, using Pt/undoped TiO₂ aerogel and Pt/TiO₂ Degussa P 25

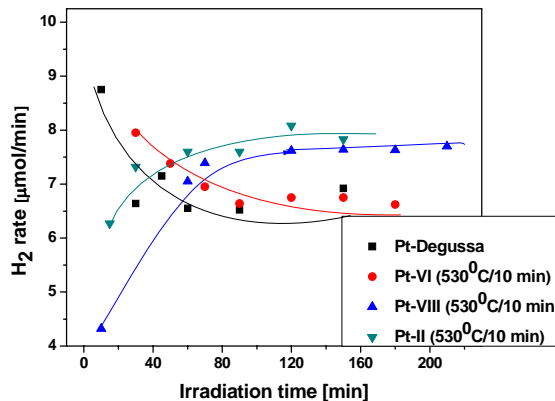


Fig.7.9. Hydrogen production at 25°C, using Pt/N(II, VI, VIII)-TiO₂ and Pt/TiO₂ Degussa P25

However, hydrogen production rate on Pt/TiO₂ Degussa P25 remains about 1.5 times higher than Pt/undoped TiO₂ aerogel.

Using Pt/N (II)-TiO₂ aerogels the hydrogen production can be increased by 12 % (Fig.7.9). These promising results encourage continuing the research in this field.

GENERAL CONCLUSIONS

- Metal (Fe, Ce, Cu) ions and non-metal (N) were used in order to dope TiO₂ aerogels. The aerogel structure was obtained by sol-gel process in acid catalysis, followed by supercritical drying with CO₂. Techniques such XRD, XPS, adsorption-desorption isotherms, ICP-MS, [OH_{surf}] determination, FTIR, TEM, SEM, Raman spectroscopy, thermogravimetry were used in order to morhostructural characterize the obtained materials;
- The type and the concentration of the doping agents, the doping methods, and temperatures and times of thermal treatment were mainly studied;
- All the obtained samples had mainly TiO₂ anatase crystalline structure (> 75%), rutile and brookite structures were also detected predominantly in Ce- and Cu - TiO₂ aerogels;
- The mean anatase particle size were between 10-24 nm, depending on the synthesis conditions;
- The position of Fe³⁺ ions was predominantly substitutional (Fe-O-Ti) and the position of N was substitutional (Ti-N-Ti) and/or interstitial, in TiO₂ lattice;
- The M-TiO₂ and N-TiO₂ aerogels had a mesoporous structure, with mean mesopores radius between 2 - 6 nm and specific surface area between 60-160 m²/g.
- The Me-TiO₂ and N-TiO₂ absorb radiations in the UV and in the VIS region of solar spectrum;
- The apparent rate constant (k_{app}) normalized with the specific surface area indicated an increase with about 60% in the case of N-TiO₂ aerogel (sample A530-10), comparing with the undoped one;
- The highest photonic efficiencies were obtained for Fe(1.8at%)-TiO₂ ($\xi = 1.59 \cdot 10^{-4}$), and N-TiO₂ (sample III) ($\xi = 1.43 \cdot 10^{-4}$);
- S_{BET} and [OH_{surf}] favored the adsorption of SA on the photocatalysts surface, and thus, increasing the photocatalytic activity. However, N in substitution position mainly induced a narrowing of the band gap from 3.04 eV to 2.80 eV and could compensate a smaller S_{BET} and [OH_{surf}]. An increasing with about 23.5% of the photonic efficiency was observed in the case of N-TiO₂, comparing with the undoped TiO₂ ;

- VIS irradiation of the N-TiO₂ (sample A530-10) determined a conversion of 68.3% of SA.
- After 5 hours of adsorption and UV irradiation, the concentration of pollutant organic compounds existing in the wastewaters (ametrine, triclosan, 1,2,3-trichlorobenzene, 2,6-dichlorophenol) decreased ~99%.
- Pt/N-TiO₂ aerogel increased the hydrogen production rate with about 12 %.

REFERENCES

1. A. Mills, C. E. H., R. H. Davies, D. Worsley, *J.Photochem. Photobiol. A: Chem* **1994**, 83, 257.
2. A. Mills, S. M., R. Davies, *J. Photochem. Photobiol. A: Chem.* **1993**, 70, 183.
3. C-Y. Hsiao, C.-L. L., D.F. Ollis, *J. Catal.* **1983**, 82, 418.
4. J. Chen, D. F. O., W.H. Rulkens, H. Bruning, *Wat. Res.* **1999**, 33, 661.
5. Kawaguchi, H., *Environ. Sci. Technol.* **1984**, 5, 471.
6. L. Muszkat, L. B., L. Feigelso, *J. Photochem. Photobiol. A: Chem.* **1995**, 87, 85.
7. N. Daneshvar, D. S., A. R. Khataee, *J. Photochem. Photobiol. A: Chem.* **2003**, 157, 111.
8. R.W. Matthews, S. R. M., *J. Photochem. Photobiol. A: Chem.* **1992**, 64, 231.
9. O. Carp, C. L. H., A. Reller, *Progress in Solid State Chemistry* **2004**, 32, 33.
10. Diebold, U., *Surface Science of titanium dioxide*. Departament of Physics, Tulane Univ.: New Orleans, **2002**.
11. <http://britneysears.ac/physics/basics/basics.htm>
12. M. Schneider, A. B., Titania-based aerogels. *Catal. Today* **1997**, 35, 339.
13. A. Sadeghzadeh Attar, M. S. G., F. Hajiesmaeilbaigi, Sh. Mirdamadi, K. Katagiri, K. Koumoto, *J. Phys. D: Appl. Phys.* **2008**, 41, 155318.
14. *Titanium Dioxide Photocatalyst*; Three Bond Technical News: Tokyo, Japan, **2004**.
15. A. Di Paola, M. A., M. Bellardita, E. Cazzanelli, L. Palmisano, *Thin Solid Films* **2007**, 515, 3527.
16. R. C. Bhave, B. I. L., *Mater. Sci. Engin. A* **2007**, 467, 146.
17. R.R. Basca, M. G., *J. Am. Ceram. Soc.* **1996**, 79, 2185.
18. W.W. So, S. B. P., K.J. Kim, C.H. Shin, S.J. Moon, *J. Mater. Sci.* **2001**, 36, 4299.
19. X. You, F. C., J. Zhang, *J.Sol-Gel Sci. Technol.* **2005**, 34, 181.
20. H. Z. Zhang, J. F. B., *J. Mater. Chem.* **1998**, 8, 2073.
21. P.S. Ha, H. J. Y., H.S. Jung, K.S. Hong, Y.H. Park, K.H. Ko, *J. Colloid Interf. Sci.* **2000**, (16), 223.
22. R. D. Shannon, J. A. P., *J. Am. Chem. Soc.* **1965**, 48, 391.
23. H. Zhang, J. F. B., *J. Phys. Chem B* **2000**, 104, 3481.
24. H. Izutsu, P. N. N., F. Mizukami, *J. Mater. Chem.* **1997**, 7, 855.
25. C. Legrand-Buscema, C. M., S. Bach, *Thin Solid Films* **2002**, 418, 79.
26. A. Karthikeyan, R. M. A., *J. Non-Cryst. Solids* **2000**, 274, 169.
27. J. Yang, J. M. F. F., *Mater. Res. Bull.* **1988**, 33, 389.
28. G. Colon, M. C. H., J.A. Navio, *Appl. Catal. A. General* **2002**, 231, 185.
29. T.L. Thompson, J. T. Y., *Chem. Rev.* **2006**, 106, 4428.
30. Henderson, M. A., *Langmuir* **1996**, 12, 5093.
31. W.S. Epling, C. H. F. P., M.A. Henderson, U. Diebold *Surf. Sci.* **1998**, 412, 333.
32. F. Pedraza, A. V., *J. Phys. Chem. Solids* **1999**, 60, 445.
33. S.K. Poznyak, A. I. K., A.I. Kulak, *J. Electroanal. Chem.* **1998**, 442, 99.
34. A. Di Paola, E. G.-L., S. Ikeda, G. Marci, B. Ohtani, L. Palmisano, *Catal. Today* **2002**, 75, 87.
35. K.T. Ranjit, B. V., *J. Photochem. Photobiol. A: Chem.* **1997**, 108, 79.
36. Z. Ambrus, N. B., T. Alapi, G. Wittmann, P. Sipos, A. Dombi, K. Mogyorosi, *Appl. Catal. B: Environ.* **2008**, 81, 27.
37. H. Wei, Y. W., N. Lun, F. Zhao, *J. Mater. Sci.* **2004**, 39, 1305.
38. A. M. T. Silva, C. G. S., G. Drazic, J. L. Faria, *Catal. Today* **2009**, 144, 13.
39. M. Hirano, C. N., K. Ota, O. Tanaike, M. Inagaki, *J. Solid State Chem.* **2003**, 170, 39.
40. S. Yin, Y. F., J. Wu, M. Aki, T. Sato, *J. Mater. Proc. Tech.* **2003**, 137, 45.
41. D. N. Furlong, C. D. P., *J. Colloid Interf. Sci* **1978**, 65, 548.
42. T. Tong, J. Z., B. Tian, F. Chen, D. He, M. Anpo, *J. Colloids Interf. Sci* **2007**, 315, 382.
43. P.N. Kapoor, S. U., S. Rodriguez, K. J. Klabunde, *J. Molecular Catal. A: Chem.* **2005**, 229, 145.
44. B. Xin, Z. R., P. Wang, J. Liu, L. Jing, H. Fu, *Appl. Surf. Sci* **2007**, 253, 4390.
45. P. Fabrizioli, T. B., M. Burgener, S. van Doorslaer, A. Baiker, *J. Mater. Chem.* **2002**, 12, 619.
46. S. Zhu, T. S., W. Liu, S. Wei, Y. Xie, C. Fan, Y. Li, *Phys. B* **2007**, 396, 177.
47. T. Lopez, J. A. M., R. Gomez, X. Bokhimi, J. A. Wang, H. Yee-Madeira, G. Pecchi, P. Reyes, *J. Mater. Chem.* **2002**, 12, 714.
48. X. Li, P. Y., C. Kutal, *New J. Chem.* **2003**, 27, 1264.
49. E. Celik, Z. G., N.F. Ak. Azem, M. Tanoglu, O. F. Emrullahoglu, *Mater. Sci. Eng. B* **2006**, 132, 258.

50. G. Colon, M. M., M. C. Hidalgo, J. A. Navio, *Appl. Catal. B: Environ.* **2006**, 67, 41.
51. J. Wang, S. U., K.J. Klabunde, *Appl. Catal. B: Environ.* **2004**, 48, 151.
52. C. Adan, A. B., M. Fernandez-Garcia, A. Martinez-Arias, *Appl. Catal. B: Environ.* **2007**, 72, 11.
53. J. Sa, C. A. A., S. Gross, J.A. Anderson, *Appl. Catal. B: Environ.* **2009**, 85, 192.
54. F. Patricia, T. B., B. Marco, S. van Doorslaer A. Baiker, *J. Mater. Chem.* **2002**, 12, 619.
55. C. Wang, C. B., D. W. Bahnemann, J. K. Dohrmann, *J. Nanoparticles Res.* **2004**, 6, 119.
56. C. Wang, C. B., D. W. Bohnemann, J. K. Dohremann, *J. Mater. Chem.* **2003**, 13, 2322.
57. N. Sijacovic-Vujicic , M. G., S. Music , M. Ivanda , S. Popovic *J. Sol-Gel Sci. Technol.* **2004**, 30, 5.
58. P.K. Robertson, D. W. B., J. M. C. Robertson, F. Wood, Photocatalytic Detoxification of Water and Air in *Environmental Photochemistry Part II*, Springer-Verlag: Berlin **2005**.
59. A. L. Linsebigler, G. L., J. T. Yates Jr., *Chem. Rev.* **1995**, 95, 735.
60. A. Inoue, E. I., *J. Phys.* **1979**, C12, 5157.
61. S. Karvinem, P. H., T.A. Pakkanen, *J. Mol. Struct.- Theochem.* **2003**, 626, 271.
62. J.A. Wang, R. L.-B., *J. Phys. Chem. B* **2001**, B 105, 9692.
63. W.J. Zhang, Y. L., S.L. Zhu, W.H. Wang, *Chem. Phys. Lett.* **2003**, 373, 333.
64. D. Beydoun, R. A., G. Low, S. McEvoy, *J. Nanoparticle Res.* **1999**, 1, 439.
65. W. Choi, A. T., M.R. Hoffmann, *J. Phys. Chem.* **1994**, 98, 13669.
66. W. Li, A. I. F., J.C. Voicic, C. Ni, S. I. Shah, *Am. Phys. Soc., Phys. Rev.* **2005**, B 72, 155.
67. Z. Zhang, C. C. W., R. Zakaria, J.Y. Ying, *J. Phys. Chem.* **1998**, B 102, 10871.
68. Z. Liu, B. G., L. Hong, H. Jiang, *J. Phys. Chem. Solids* **2005**, 66, 161.
69. Pichat, P., *Photocatalytic Degradation of Pollutants in Water and Air: Basic Concepts and Applications*. Marcel Dekker, Inc: **2003**.
70. J. Araña, O. G. D., M. Miranda Saracho, J.M. Doña Rodriguez, J.A. Herrera Melián, J. Pérez Peña, *Appl. Catal. B: Environ.* **2001**, 32, 49.
71. J. A. Navio, G. C., M. Macias, C. Real, M. I. Litter, *Appl. Catal. A: General* **1999**, 177, 111.
72. J. Xiao, T. P., R. Li, Z. Peng, C. Yan, *J. Solid State Chem.* **2006**, 179, 1161.
73. Q. Yan, X. S., Z.-Y. Huang, C.-C. Ge, *J. European Ceramic Soc.* **2006**, 26, 915.
74. R. Asahi, T. M., T. Ohwaki, K. Aoki, Y. Taga, *Sci.* **2001**, 293, 269.
75. J. S. Jang, H. G. K., S. M. Ji, S. W. Bae, J. H. Jung, B. H. Shon, J. S. Lee, *J. Solid State Chem.* **2006**, 179, 1067.
76. L. Lin, R. Y. Z., J.L.Xie, Y.X. Zhu, Y.C.Xie, *Appl. Catal. B: Environ.* **2007**, 76, 196.
77. T. Horikawa, M. K., T. Tomida, *Chem. Phys.* **2008**, 110, 397.
78. C. Feng, Y. W., Z. Jin, J. Zhang, S. Zhang, Z. Wu, Z. Zhang, *New J. Chem.* **2008**, 32, 1038.
79. T. Morikawa, Y. I., T. Ohwaki, *Appl. Catal. A: General* **2006**, 314, 123.
80. S.A. Chambers, S. H. C., V. Shutthanandan, S. Thevuthasan, M. K. Bowman, A.G. Joly, *Chem. Phys.* **2007**, 339, 27.
81. S. Sato, R. N., S. Abe, *Appl. Catal. A: General* **2005**, 284, 131.
82. Y.Q. Wang, X. J. Y., D. Z. Sun, *J. Hazardous Mater.* **2007**, 144, 328.
83. C. D. Valentin, E. F., G. Pacchioni, A. Selloni, S. Livraghi, M.C. Paganini, E. Giannello, *Chem. Phys.* **2007**, 339, 44.
84. S. Livraghi, M. R. C., E. Giannello, G. Magnacca, M.C. Paganini, G. Cappelletti, C. L. Bianchi, *J. Phys. Chem. C* **2008**, 112, 17244.
85. Y. Huang, Z. X., Y. Zhongyi, T. Feng, F. Beibei, H. Keshan, *Chin. J. Chem. Eng.* **2007**, 15, 802.
86. D. Li, N. O., S. Hishita, T. Kolodiaznyi, H. Haneda, *J. Solid State Chem.* **2005**, 178, 3293.
87. F. Peng, L. C., H. Yu, H. Wang, J. Yang, *J. Solid State Chem.* **2008**, 181, 130.
88. Y. Nosaka, M. M., J. Nishino, A. Y. Nosaka, *Sci. Technol. Adv. Mater.* **2005**, 6, 143.
89. V. Gombac, L. D. R., A. Gasparotto, G. Vicario, T. Montini, D. Barreca, G. Balducci, P. Fornasiero, E. Tondello, M. Grazini, *Chem. Phys.* **2007**, 339, 111.
90. Y. Xie, Q. Z., X. J. Zhao, Y. Li, *Catal. Lett.* **2007**, 118, 231.
91. Y. Nakano, T. M., T. Ohwaki, Y. Taga, *Chemical Physics* **2007**, 339, 20.
92. S. Sakthivel, M. J., H. Kisch, *J. Phys. Chem. B* **2004**, 108, 19384.
93. A. V. Emeline, V. N. K., V. K. Rybchuk, N. Serpone, *Int. J. Photoenergy* **2008**, doi:10.1155/2008/258394.
94. S. Sakthivel, H. K., *Chem. Phys. Chem.* **2003**, 4, 487.
95. J. Chen, L.-B. L., F. Q. Jing, *J. Phys. Chem* **2001**, 62, 1257.
96. V.N. Kuznetsov, N. S., *J. Phys. Chem. B* **2006**, 110, 25203.
97. A. Brucato, F. G., *J. Adv. Oxid Technol.* **1999**, 4, 47.
98. Herrmann, J. M., *Catal. Today* **1999**, 53, 115.
99. M.A. Fox, M. T. D., *Chem. Rev.* **1993**, 93, 341.
100. J. Arana, J. M. D.-R., O. Gonzalez-Diaz, E. Tello Rendon, J.A. Herrera Melian, G. Colon, J.A. Navio, J. Perez Pena, *J. Mol. Catal. A: Chem.* **2004**, 215, 153.
101. Y. Xu, H. C., Z. X. Zeng, B. Lei, *Appl. Surf. Sci.* **2006**, 252, 8565.
102. H. S. Park, D. H. K., S. J. Kim, K. S. Lee, *J. Alloys Comp.* **2006**, 415, 51.

103. X. Fua, J. L., X. Wang, D. Y.C. Leungb, Z. Dinga, L. Wu, Z. Zhang, Z. Lia, X. Fua, *Int. J. Hydrogen Energy* **2008**, 33, 6484.
104. F. Alonso, P. R., F. Rodríguez-Reinoso, J. Ruiz-Martínez, A. Sepúlveda-Escribano, M. Yus, *J. Catal.* **2008**, 260, 113.
105. M. Ikeda, Y. K., Y. Yakushijin, S. Somekawa, P. Ngweniform, B. Ahmmad, *Catal. Commun.* **2007**, 8, 1943.
106. I. Djerdj, A. M. T., *J. Alloys Comp.* **2006**, 413, 159.
107. N. Aldea, E. I., *Comput. Phys. Commun.* **1990**, 60, 155.
108. http://en.wikipedia.org/wiki/Raman_spectroscopy
109. J. Xua, L. L., Y. Yana, H. Wang, X. Wangb, X. Fub, G. Li, *J. Colloid Interf. Sci.* **2008**, 318, 29.
110. <http://www.unl.edu/CMRAcfem/temoptic.htm>
111. http://en.wikipedia.org/wiki/Inductively_coupled_plasma_mass_spectrometry
112. http://en.wikipedia.org/wiki/Gas_chromatography-mass_spectrometry
113. http://en.wikipedia.org/wiki/Fourier_transform_infrared_spectroscopy
114. J. A. Rob van Veen, F. T. G. V., G. Jonkers, *J. Chem. Soc., Chem. Commun.* **1985**, 1656.
115. <http://en.wikipedia.org/wiki/Thermogravimetry>
116. N. Guettai, H. A. A., *Desalination* **2005**, 185, 439.
117. S. M. Ould-Mame, O. Z., M. Bouchy, *Int. J. Photoenergy* **2000**, 2, 59.
118. G. Niac, V. V., I. Baldea, M. Preda, *Formule, tabele si probleme de chimie fizica*. Dacia: Cluj-Napoca, **1984**.
119. M. Montalti, A. C., L. Prodi, M. T. Gandolf, *Handbook of Photochemistry*. CRC Press: New York, **2006**.
120. J. Zhou, Y. Z., X.S. Zhao, A.K. Ray, *Ind. Eng. Chem. Res.* **2006**, 45, 3503.
121. J.C. Colmenares, M. A. A. a., A. Marinas, J.M. Marinas, F.J. Urbano, *Appl. Catal. A: General* **2006**, 306, 120.
122. M. Salmi, N. T., R.-J. Lamminmaki, S. Karvinen, V. Vehmanen, H. Lemmetyinen, *J. Photochem. Photobiol. A: Chem.* **2005**, 175, 8.
123. C. Wang, R. P., J.K. Dohrmann, D.W. Bahnemann, *C. R. Chim.* **2006**, 9, 761.
124. A. Kumbhar, G. C., *J. Nanoparticle Res.* **2005**, 7, 489.
125. J. H. Jho, D. H. K., S.-J. Kimb, K. S. Lee, *J. Alloys Comp.* **2008**, 459, 386.
126. A. Di Paola, G. C., M. Addamoia, M. Bellardita, R. Campostrini, M. Ischia, R. Ceccato, L. Palmisano, *Colloids Surf. A: Physicochem. Eng. Aspects* **2008**, 317, 366.
127. M. S. Nahar, K. H., S. Kagaya, *Chemosphere* **2006**, 65, 1976.
128. Y. Wang, H. C., Y. Hao, J. Ma, W. Li, , *J. Mater. Sci* **1999**, 34, 3721.
129. J. A. Wang, R. L.-B., T. Lopez, A. Moreno, R. Gomez, O. Novaro, X. Bokhimi, *J. Phys. Chem. B* **2001**, 105, 9692.
130. Z. H. Wang, J. G. L., H. Kamiyama, M. Katada, N. Ohashi, Y. Moriyoshi, T. Ishigaki, *J. Am. Chem. Soc.* **2005**, 127, 10982.
131. X. H. Wang, J. G. L., H. Kamiyama, M. Katada, N. Ohashi, Y. Moriyoshi, T. Ishigaki, *J. Am. Chem. Soc.* **2005**, 127, 10982.
132. X. H. Wang, J. G. L., H. Kamiyama, Y. Moriyoshi, T. Ishigaki, *J. Phys. Chem. B* **2006**, 110, 6804.
133. D. Y. Wang, H. C. L., C.C Yen, *Thin Solid Films* **2006**, 515, 1047.
134. X. Zhang, M. Z., L. Lei, *Catal. Commun.* **2006**, 7, 427.
135. F. B. Li, X. Z. L., M. F. Hou, K. W.Cheah, W. C. H. Choy, *Appl. Catal. A: General* **2005**, 285, 181.
136. Y. Xie, C. Y., *Appl. Catal. B: Environ.* **2003**, 46, 251.
137. G. Li, C. L., Y. Liu, *Appl. Surf. Sci.* **2006**, 253, 2481.
138. C. Liu, X. T., C. Mo, Z. Qiang, *J. Solid State Chem.* **2008**, 181, 913.
139. A. Barau , M. C., M. Gartner, V. Danciu, V. Cosoveanu, I. Marian, *Mater. Sci. Forum* **2005**, 311, 492-493.
140. V. Danciu, V. C., A. Peter, I. Marian, P. Marginean, E. Indrea, *Annals West Univ. Timisoara, Series Chem.* **2004**, 13, 75.
141. K. Chhor, J. F. B., C. Colbeau-Justin, *Mater. Chem. Phys.* **2004**, 86, 123.
142. J. Rouquerol, K. R., K. Sing, *Adsorption by powders and porous solids*. Academic Press **1999**.
143. F. Iacomi, D. M., M. N. Grecu, D. Macovei, I. V. Simiti, *Surf. Sci.* **2007**, 601, 2692.
144. J. Zhua, F. C., J. Zhang, H. Chenb, M. Anpob, *J. Photochem. Photobiol. A: Chem.* **2006**, 180, 196.
145. T. K. Ghora, S. K. B., P. Pramanik, *Appl. Surf. Sci.* **2008**, 254, 7498.
146. C. Hu, Y. Z. W., H.X. Tang, *Appl. Catal. Part B: Environ.* **2001**, 35, 95.
147. M. Descotes, F. M., N. Thromat, C. Beaucaire, M. Gautier-Soyer, *Appl. Surf. Sci.* **2000**, 165, 288.
148. G. Busca , G. R., J.M. G. Amores , V.S. Escrivano , P. Piaggio, *J. Chem. Soc. Faraday Trans.* **1994**, 90, 3181.
149. M. Gotic , M. I., A. Sekulic , S. Music , S. Popovic , A.Turkovic , K. Furic, *Mater. Lett.* **1996**, 28, 225.
150. Y.H. Zhang, C. K. C., J.F. Porter, W. Guo, J. Mater. Res., *J.Mater. Res.* **1998**, 13, 2602.
151. S. Kelly, F. H. P., M. Tomkiewicz, *J. Phys. Chem.* **1997**, 101, 2730.
152. H. C. Choi , Y. M. J., S. B. Kim, *Vibrational Spectroscopy* **2005**, 37, 33.
153. L. Baia, A. P., V. Cosoveanu, E. Indrea, M. Baia, J. Popp, V. Danciu, *Thin Solid Films* **2006**, 511.

154. L. Baia , M. B., A. Peter , V. Cosoveanu , V. Danciu *J. Optoelectr. & Advanced Mater.* **2007**, 9, 668.
155. L.Shun-Xing, Z. F.-Y., C. Wen-Lian, H. Ai-Qin, X. Yu-Kun, *J. Hazardous Mater. B* **2006**, 135, 431.
156. S. Tunesi, M. A., *J. Phys. Chem.* **1991**, 95, 3399.
157. Y. Tanaka, M. S., *J. Sol-Gel Sci. Tech.* **2002**, 22, 83
158. J. Aguado-Serrano, M. L. R.-C., *Micropor. Mesopor. Mat.* **2006**, 88, 205.
159. J.M. Coronado, A. J. M., A. Martinez-Arias, J.C. Conesa, J. Soria, *J. Photochem. Photobiol. A: Chem.* **2002**, 150, 213.
160. H. K. Shon, S. V., J. Kim, H. Ngo, *Korean J. Chem. Eng.* **2007**, 24, 618
161. R.S. Sonawane, B. B. K., M.K. Dongare, *Mater. Chem. Phys.* **2004**, 85, 52.
162. K. Nishijima, B. O., X. Yan, T. Kamai, T. Chiyoya, T. Tsubota, N. Murakami, T. Ohno, *Chem. Phys.* **2007**, 339, 64.
163. P. G. Wu, C. H. M., J. K. Shang, *Appl. Phys. A* **2005**, 81, 1411.
164. X. Qiu, C. Burda, *Chem. Phys.* **2007**, 339, 1.
165. C.J. Doss, R. Z., *Phys. Rev. B* **1993**, 48, 15626.
166. Nesheva, D., *J. Opto. & Adv. Mater* **2005**, 7, 185.
167. X. Chen, Y. L., A.C.S. Samia, C. Burda, *Adv. Funct. Mater.* **2005**, 15, 41.
168. H. Chen, A. N., W. Wen, J. Graciani, Z. Zhong, J. C. Hanson, E. Fujita, J. A. Rodriguez, *J. Phys. Chem. C* **2007**, 111, 1366.
169. J. H. Xu, W. L. D., J.X. Li, Y. Cao, H.X. Li, H. He, K. Fan, *Catal. Commun.* **2008**, 9, 146.
170. R. Nakamura, T. T., Y. Nakato, *J. Phys. Chem. B* **2004**, 108, 10617.
171. N.C. Saha, H. G. T., *J. Appl. Phys., J. Appl. Phys.* **1992**, 72, 3072.
172. S. Badrinarayanan, S. S., A.B. Mandale, *J. Electron Spectrosc. Relat. Phenom.* **1989**, 49, 303.
173. H. X. Li, J. X. L., Y.I. Huo, *J. Phys. Chem. B* **2006**, 110, 1559.
174. Y.G. Sheng, Y. X., D. Jiang, L. Liang, D. Wu, Y. Sun, *Int. J. Photoenergy* doi:10.155/2008/563949.
175. E. Gyorgy, A. P. d. P., P. Serra, J.L. Morenza, *Surf. Coat. Technol.* **2003**, 173, 265.
176. Gopinath, C. S., *J. Phys. Chem. B* **2006**, 110, 7079.
177. X. B. Chen, C. B., *J. Phys. Chem. B* **2004**, 108, 15446.
178. F. Esaka, K. F., H. Shimada, M. Imamura, N. Matsubayashi, H. Sato, A. Nishijima, A. Kawana, H. Ichimura, T. Kikuchi, *J. Vac. Sci. Technol. A* **1997**, 15, 2521.
179. P. M. Kumar, S. B., M. Sastry, *Thin Solid Films* **2000**, 358, 122.
180. T. Srithawong, S. L., S. Chavadej, *Int. J. Hydrogen Energy* **2008**, 33, 5947.
181. *Handbook of X-ray Photoelectron Spectroscopy*. Perkin-Elmer Corp.: Waltham, MA, **1992**.
182. J. Guillot, A. J., L. Imhoff, B. Domenichini, O. Heintz, S. Zerkout, A. Mosser, S. Bourgeois, *Surf. Interf. Anal.* **2002**, 34, 577.
183. C. Di Valentin, G. F. P., A. Selloni, S. Livraghi, E. Giannello, *J. Phys. Chem. B* **2005**, 109, 11414.
184. J. Yu, J. X., B. Cheng, S. Liu, *Appl. Catal. B: Environ.* **2005**, 60, 211.
185. R. P. Netterfield, P. J. M., C.G. Pacey, W.G. Sainty, D.R. McKenzie, G. Auchterlonie, *J. Appl. Phys.* **1989**, 66, 1805.
186. A. Pashutski, M. F., *Surf. Sci.* **1989**, 216, 395.
187. B. Erdem, R. A. H., G. W. Simmons, E. D. Sudol, V. L. Dimonie, M. S. El-Aasser, *Langmuir* **2001**, 17, 2664.
188. M. Andersson, L. O., S. Ljungstron, A. Palmqvist, *J. Phys. Chem. B* **2002**, 106, 10674.
189. M. Inagaki, Y. N., M. Hirano, Y. Kobayashi M. Toyoda, *Int. J. Inorg. Mater.* **2001**, 3, 809.
190. A.J. Sequeira, L. T. T., *J. Chromatographic Sci.* **1991**, 29, 351.
191. <http://www.chemicaland21.com/specialtychem/finechem/1> TRICHLOROBENZENE.htm
192. A. Claver, P. O., L. Rodriguez, J. L. Ovelloiro, *Chemosphere* **2006**, 64, 1437.
193. C. Tixier, H. P. S., S. Canonica, S.R. Muller, *Environ. Sci. Technol.* **2002**, 36, 3482.
194. H. Singer, S. M., C. Texier, L. Pillonel, *Environ. Sci. Technol.* **2002**, 36, 4998.
195. A. Patsoura, D. I. K., X. E. Verykios, *Appl. Catal. B: Environ.* **2006**, 64, 171.